World Academy of Science, Engineering and Technology
International Journal of Civil and Architectural Engineering
Vol:17, No:6, 2023

Land Use/Land Cover Mapping Using Landsat 8 and Sentinel-2 in a Mediterranean Landscape

M. Vogiatzis, K. Perakis

***Abstract*—**Spatial-explicit and up-to-date land use/land cover information is fundamental for spatial planning, land management, sustainable development, and sound decision-making. In the last decade, many satellite-derived land cover products at different spatial, spectral, and temporal resolutions have been developed, such as the European Copernicus Land Cover product. However, more efficient and detailed information for land use/land cover is required at the regional or local scale. A typical Mediterranean basin with a complex landscape comprised of various forest types, crops, artificial surfaces, and wetlands was selected to test and develop our approach. In this study, we investigate the improvement of Copernicus Land Cover product (CLC2018) using Landsat 8 and Sentinel-2 pixel-based classification based on all available existing geospatial data (Forest Maps, LPIS, Natura2000 habitats, cadastral parcels, etc.). We examined and compared the performance of the Random Forest classifier for land use/land cover mapping. In total, 10 land use/land cover categories were recognized in Landsat 8 and 11 in Sentinel-2A. A comparison of the overall classification accuracies for 2018 shows that Landsat 8 classification accuracy was slightly higher than Sentinel-2A (82,99% vs. 80,30%). We concluded that the main land use/land cover types of CLC2018, even within a heterogeneous area, can be successfully mapped and updated according to CLC nomenclature. Future research should be oriented toward integrating spatiotemporal information from seasonal bands and spectral indexes in the classification process.

***Keywords*—**Land use/land cover, random forest, Landsat-8 OLI, Sentinel-2A MSI, Corine Land Cover.

I. Introduction

LAND use/land cover earth observation mapping and thematic products are key baseline data for monitoring land changes, natural biophysical reserves, and data inputs for spatially explicit models of climate change, crop production, and ecosystem resources. Remarkably, in 2015 [21], United Nations Agenda 2030 on sustainable development stressed the importance of new earth observations and geospatial data to promote effective monitoring of its targets and goals.

Over the last decade, free access on medium-high spatial resolution satellite imagery, such as Landsat and Sentinel, facilitates the development of new satellite-based applications and the production of up-to-date improved geospatial land cover data products at global, national, regional and local scales.

In Europe, CORINE Land Cover (CLC) provides harmonized and comprehensive maps of land cover and land use change at European level [1]. The program (nowadays "Copernicus Land Cover") was established by the European Commission (EU) in 1990 for facilitating policy making at European level. The most recent CLC2018 comprises of 44 thematic classes at the third level with a minimum mapping unit (MMU) of 25 Ha for areal features, and 5 Ha for changes, respectively. It is an excellent tool for strategic analysis and planning at European level. However, CLC's thematic content comprises a mixture of land cover and land use classes. In addition, its MMU serves well the needs of the European Union but is not suited for national or regional planning activities [2]. Another disadvantage is that CLC approach heavily relies on visual interpretation of medium resolution satellite imagery and various mapping approaches may be employed by national agencies across EU member states [3]. Therefore, there is a strong need to develop and test automated approaches for mapping land use/land cover at national or local level.

A variety of classification approaches (unsupervised, supervised, parametric, non-parametric, object-oriented) have been developed and applied to derive land cover information with different degree of success. However, per-pixel classification approaches remain the most popular in analysis of satellite-derived imagery [4].

In this study, we apply Random Forest (RF) classifier to derive land use/land cover information [5]. RF is a well-known machine-learning classifier, which has been used and tested in different approaches for land use/land cover mapping in the last decade (e.g. [6]-[8]). Furthermore, such classifiers have already been used in operational initiatives for land cover classification (e.g. USGS Land Change Monitoring, Assessment, and Projection (LCMAP) [9] and USGS National Land Cover Database (NLCD) [10]). However, classification accuracy depends on the satellite imagery and the classification algorithm being used, and the nature of training data as well [11].

In supervised approaches, reference data are required to characterize the variability of land cover across space and time and serve as reference dataset for training and validating classification models. Suitable reference data are a fundamental requirement in supervised image classification [12]. We use existing authoritative geospatial datasets of higher accuracy as a pool for training and validation. The reference datasets span forestlands, cultivated fields, discontinuous urban fabric and built-up areas, road network

M. Vogiatzis is Ph.D. candidate with the Department of Planning and Regional Development, School of Engineering, University of Thessaly, Pedion Areos, Volos, 38334, Greece and Director of Forest Maps and Mapping of Natural Environment at Hellenic Cadastre, 136 Tsimiski Ave., 54621 Thessaloniki, Greece (phone: +30 2310370524; fax: +30 2310370513; e-mail: vogiatzismimis@gmail.com).

K. Perakis is Professor of Remote Sensing and Statistical Applications at the Department of Planning and Regional Development, School of Engineering, University of Thessaly, Pedion Areos, Volos, 38334, Greece.

and natural habitats. The classification scheme of land cover classes is based on the third level of CLC nomenclature. Based on CLC2018 land use/land cover distribution, a stratified random sampling scheme is deployed to train the classifier and access classification accuracy.

In this paper, we explore the relationship between classification performance and satellite imagery of different spectral and spatial resolutions. The study investigates the performance of RF classification using Landsat 8 and Sentinel-2A across a heterogeneous Mediterranean watershed, based on the same available geospatial reference data. We evaluate the mapping approach and address the following research questions:

- How does spatial and spectral resolutions of satellite imagery impact classification accuracy, and
- How does the land use/land cover map compare to the CLC2018 Land Cover product?

II. Study Area

The study area covers a watershed in Makedonia Region of Northern Greece lying East of Thessaloniki city (40˚40΄56,49N and 23˚18΄21,15E, WGS84) at a distance of 41,6 km (Fig. 1).

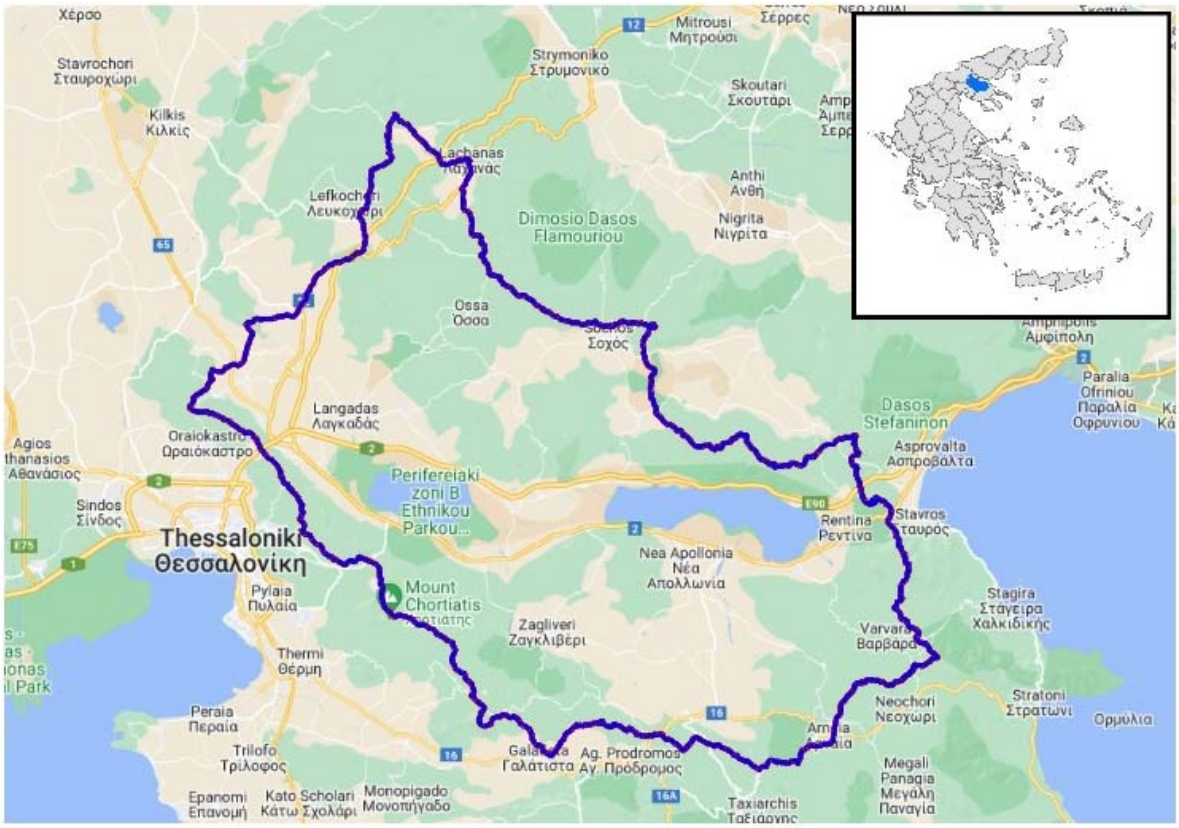

Fig. 1 Location of study area (in blue)

The watershed is surrounded by mountains in the North (Mount Krousia) and in the South (Mount Cholomontas), by hills in the West and by Rentina Gorge and Kerdylia mount in the East. It has a total area of 190.285 Ha. Its elevation ranges from 35 m to 1.129 m. At the center of the watershed, there are two lakes (Koronia and Volvi). The watershed is drained at these lakes and then at sea in the East, through Richios creek, which crosses Rentina Gorge.

The two lakes along with their wetlands have been listed as a Wetland of International Importance by the Ramsar Convention enforced in 1975 (GR005: 16.388 Ha) [22]. Along with the valley of Rentina Gorge, they have been designated as Special Conservation Zones within the Natura2000 network (GR1220001 and GR1220003: 28.734,90 Ha) in 2017 [23]. These protected areas constitute a unique complex of interconnected natural ecosystems of lakes, seasonal creeks, channels, riparian forests, shrubs, wet meadows and fields

A third broader zone, designated as Special Protected Zone (GR1220009) under Council Directive 79/409/EEC on the conservation of wild birds, surrounds the above-protected areas. It encompasses an area of 160.628,72 Ha, almost two thirds of the total watershed area. A number of important habitats for rare and endangered species exist within this zone.

At the southernmost end of the watershed, on the slopes of mount Cholomontas, there is a portion of another protected area (GR1270001). It has an area of 15.651,14 Ha dominated by beech, oak and pine forests.

The climate is considered temperate (Csa-Mediterranean mainland) with warm and dry summers and cool winters. The mean annual temperature is 22,6 °C in summer and about 4 °C

in winter. The mean annual rainfall is 593 mm according to the records of the last 40 years.

The main land cover types in the watershed include forestlands (coniferous, broadleaf, shrubs and woodlands: 80.000 Ha), various crops (irrigated and non-irrigated arable land, plantations of fruit and olive trees), artificial surfaces (small towns, roads and built-up areas), lake water, and wetlands (Fig. 2).

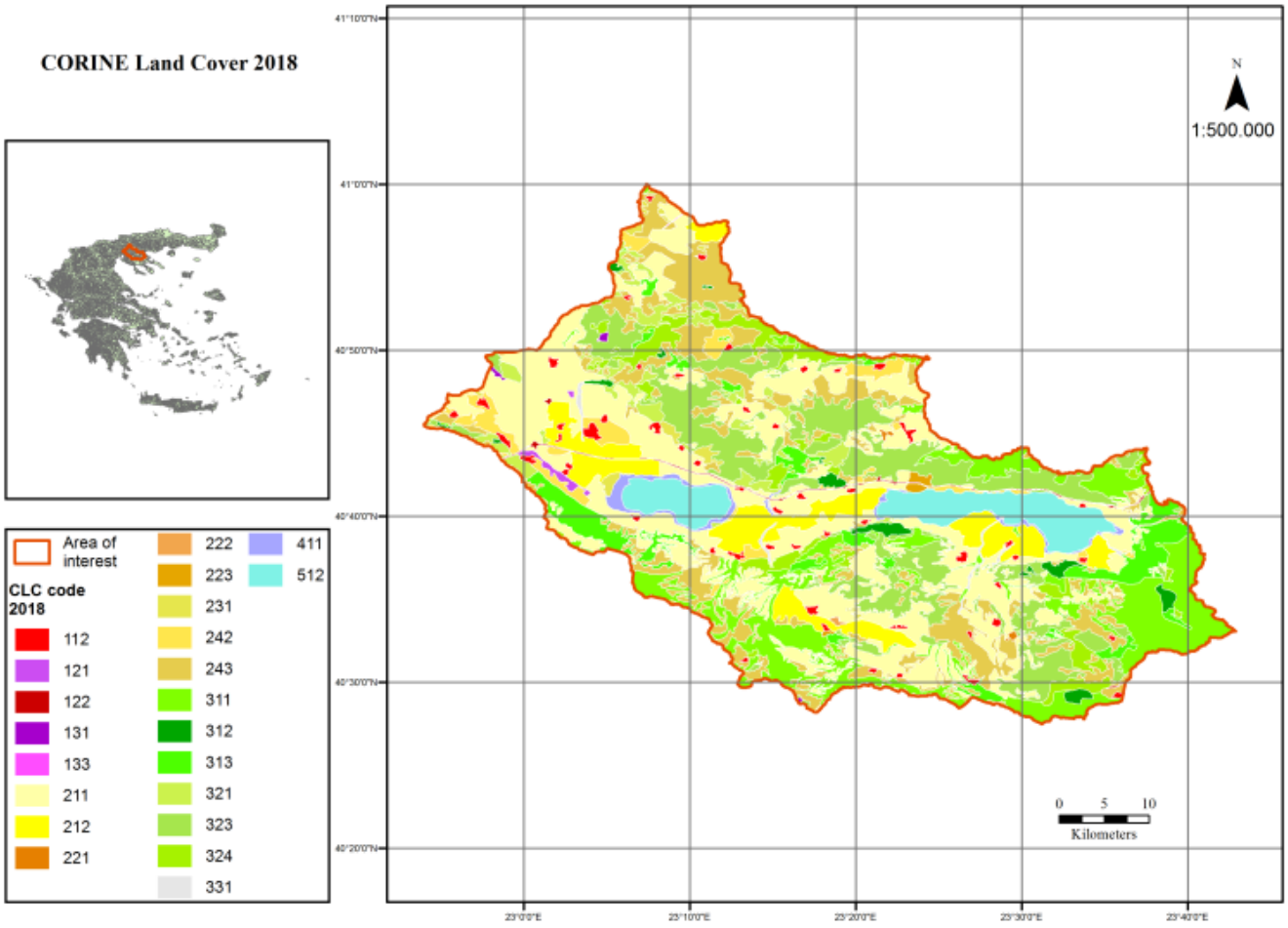

Fig. 2 CLC2018 Land use/land cover types

According to CLC2018, 49,28% of the watershed is under agricultural use while forestlands occupy 42,04%, water 5,46%, discontinuous urban fabric 1,31%, wetlands 1,17%, and developed areas comprise 0,33%. Most of the land under agricultural use is used as cropland (93,770 Ha) while the area of perennial crops such as fruit and olive tree plantations and vineyards as well, account for only 0,65%. Irrigated lands cover 14,27% while non-irrigated 50,97% of croplands. Approximately 30,98% of forestlands are broadleaf forests, 2,73% are pine forests, 12,04% mixed forests, 36,80% shrubs and 10,10% transitional woodlands. These characteristics designate an ideal representative study area to test land cover classification performance in a hierarchical framework.

III. Material and Methods

A. Satellite Imagery

Landsat 8 Operational Land Imager (OLI) surface reflectance (C2L2) data were obtained from the Unites States Geological Survey web site [13]. Two scenes (path/row: 183/032 and 184/032) required to cover entirely the study area. Following a search, cloud free (< 10%) scenes were selected for dry summer season. The scenes were acquired in 1 July 2018 and 22 June 2018 respectively. A mosaic containing six bands (blue, green, red, near-infrared (NIR), shortwave infrared (SWIR) 1, SWIR 2) was created at the study area limits.

Sentinel-2A MSI imagery was downloaded from the Sentinels Scientific Data Hub [14]. Each product consists of 100x100 sq. km orthorectified granules or tiles. Four cloud free (< 10%) granules were required to cover entirely the study area (Table I).

The 13 spectral bands of Sentinel-2A span from the visible to SWIR spectrum, at 10 m, 20 m and 60 m spatial resolutions. The bands at 60 m spatial resolution are dedicated primarily for detecting atmospheric features and were therefore excluded from the analysis [15]. A mosaic of ten bands (2-8, 8A, 11 and 12) was created at the study area limits. In order to unify the spatial resolution of the 20 m and 10 m bands, a

downscale procedure by nearest neighbor interpolation was followed, which has been shown to perform very satisfactory compared to other approaches [16].

TABLE I
SENTINEL-2A SCENES

Date	Granule
03-07-2018	L2A_T34TFK_A015820_20180703T092224
	L2A_T34TFL_A015820_20180703T092224
	L2A_T34TGK_A015820_20180703T092224
	L2A_T34TGL_A015820_20180703T092224

Both Landsat 8 and Sentinel-2A image scenes are spatially registered in Universal Transverse Mercator (UTM)/World Geodetic System 1984 (WGS84) projection.

B. Land Cover Reference Data

We utilized expert knowledge from ancillary data during our entire process. We compiled many ancillary data from different sources and used them for land use/land cover mapping and post processing to increase mapping accuracy and consistency. Existing geospatial reference data were acquired from Hellenic Cadastre, the largest provider of geospatial data in Greece (Table II).

To identify agricultural fields and especially plantation trees (fruit, olive trees, etc.) along with information on irrigated lands we used data provided by the Land Parcel Identification System (LPIS). LPIS together with the Geospatial Aid Application (GSAA) data, tracks individual claims for subsidies made by the farmers and provides detailed information of agricultural land holdings on the parcel level [17]. Both data sources, LPIS and GSAA represent an integral element for the implementation of the European Union (EU) Common Agricultural Policy (CAP).

Information regarding habitats was retrieved from national Natura2000 database. Through its processing, we gain valuable spatial information on the species dominated the wetlands within the study area.

According to Forest Maps, forestlands cover an area of 94.953 Ha, i.e. 0,49% of the study area. Forest Maps are high-resolution diagrams depicting forested and non-forested lands, according to the current legislative framework of Greece.

TABLE II
Geospatial Reference Datasets

a/a	Data	Source	Date	Scale
1.	Agricultural fields	LPIS	2018	1:5.000
2.	Habitats	Natura2000	2017	1: 5.000
3.	Urban zones	Forest Map	2021	1:5.000
4.	Forest/Non-Forest lands	Forest Map	2021	1:5.000
5.	Forest Stands	Forest Management Plans	2007-2018	1:20.000
6.	Built-up areas and road network	Cadastral database	2021	1:1.000

Forest Maps have been developed in the last 20 years by Hellenic Cadastre in cooperation with the Greek Forest Service. Their production is based on Very-High-Resolution (VHR) aerial orthoimagery at spatial resolution of 1 m. Land status (forest/ non-forest) and delineation of their respective boundaries is based on aerial photo photointerpretation taking in account a plethora of data (administrative deeds, judicial decisions, historical land distribution diagrams, urban zones, and field data) [18]. However, Forest Maps lack information on dominant vegetation and species, since their scope of works by default was forestlands delineation and land tenure determination. This kind of information was acquired by processing existing forest management plans at the stand level. These plans cover only an area of 33.529 Ha, i.e. 35,31% of forestlands according to official Forest Maps and 17,61% of the study area. Based on this information, we strongly infer that the rest of forestlands are unmanaged.

Geospatial data regarding road network and discontinued built-up areas either industrial or residential were derived from current cadastral database.

All these reference data were processed having the same projection with satellite imagery. A learning database was developed of existing geospatial data that provides information either on land cover type or per parcel. This learning database was used both in the selection of training data and validation points.

C. CLC2018 Validation

The CLC2018 classification scheme at the third level identifies 22 classes within the study area (Table III). Our goal was to validate the pre-defined classes of CLC2018 in terms of their spectral, spatial and thematic accuracy. However, the validation of CLC2018 product is a difficult task due to its large number of land cover/land cover classes. Moreover, there are mixed classes, which consist of spectrally heterogeneous land cover types [19]. For instance, classes with land use/land cover codes 243 (Land principally occupied by agriculture, with significant areas of natural vegetation) and 324 (Transitional woodland/shrub) cannot be spectrally discriminated, based on aerial or satellite data. These classes commonly include a mixture of land cover types, such as fields, natural grasslands, shrubs and broad-leaved trees with different spectral characteristics. In addition, land use/land cover type (Pastures, code 231) is rare at Mediterranean landscapes. Based on current CLC18 classes, we randomly selected points using a gridded stratified random approach, proportional to each class area, for 95% accuracy. The total sample is 2.779 (Table III).

Sampling plots were defined at the pixel spatial resolution (30 x 30 m) of Landsat imagery. Each random point was located at the center of the respective pixel using a gridded fishnet on Landsat pixels. Each plot was divided into 3 x 3 pixels to coincide with Sentinel-2A spatial resolution (10 m). Google Earth high-resolution (2019) imagery visual interpretation per plot, based on physiognomic attributes (color, shape, size, pattern and texture), was applied supported by land cover reference data. The procedure resulted in the identification of 15 classes (112, 121, 122, 131, 211, 212, 221, 222, 223, 311, 312, 323, 411, 511 and 512). Based on interpretation, each plot was assigned to one of the above classes according to CLC nomenclature. The populated

samples were added to the learning database.

TABLE III
CLC2018 LEVEL 3 CLASSES AND SAMPLE DISTRIBUTION

a/a	Code	Class	Area (Ha)	# Sample points
1	112	Discontinuous urban fabric	2.501,82	37
2	121	Industrial or commercial zones	443,74	6
3	122	Road and rail networks and associated land	752,93	11
4	131	Mineral extraction sites	161,03	2
6	211	Non-irrigated arable land	47.798,64	699
7	212	Permanently irrigated arable land	13.381,79	196
8	221	Vineyards	129,21	2
9	222	Fruit trees	71,24	1
10	223	Olive trees	404,69	6
11	231	Pastures	1.092,00	16
12	242	Complex cultivation patterns	5.083,44	74
13	243	Land principally occupied by agriculture	25.811,16	378
14	311	Broadleaf forest	24.783,86	362
15	312	Coniferous forest	2.180,58	31
16	313	Mixed forest	9.630,05	141
17	321	Natural grasslands	5.878,48	85
18	323	Sclerophyllous vegetation	29.441,81	431
19	324	Transitional woodland/shrub	8.082,38	117
20	331	Beaches, dunes, sand	572,60	8
21	411	Inland marshes	1.660,55	24
22	512	Water bodies	10.397,98	152
		Total	190.285,09	2.779

D.Classification

The supervised classifier RF was applied on the entire study area for image classification. The RF classifier has becoming increasingly common in land use/land cover applications. All procedures in this study were implemented using Erdas Imagine 2018.

We tested the utility of a single-date (summer 2018) classification inputs for land use/land cover classification. The aforementioned single-date spectral bands from Landsat 8 and Sentinel-2A images were used. We acknowledged that many other different combinations of spectral and temporal features or approaches could be used. We decided to use the aforementioned features in our analysis, to access the maximum of land cover variability.

We defined a set of training polygons by random sampling 70% of the points selected for CLC2018 class validation. These data are then used to train supervised classification models for most of the important land use/land cover classes. The remaining 30% of samples was used for validation. Training polygons were manually generated at locations of sample plots taking in account that cover types should be spectrally homogeneous. For this reason, in many cases, we forced to generate training polygons away from sample locations. We avoided long and thin training polygons. Small polygons tend to be prone to edge effect. Moreover, we selected more training polygons in areas where land cover reference data were missing or in highly heterogeneous areas, in order to increase classification accuracy. The generation of training data in areas where land cover reference data are missing proved to be an issue. Their selection was based on our expert knowledge of the study area in relation to spectral data. The total number of pixels used for training was 48.717 (2,30% of total imagery pixels) for Landsat-8 and 389.099 (2,04%) for Sentinel-2A.

Numerous iterations of RF with different combinations of land use/land cover classes were implemented on both types of imagery. Land cover classification accuracy is affected by the number of classes identified. Overall classification accuracy decreases by increasing the number of classes [20]. Therefore, we removed small area classes, such as 121, 221, 222, and 223 from Sentinel-2A classifications. The first one along with land cover type 112 formed a new class, named as "Artificial Surfaces" while the rest appended to 211. We finally identified 10 classes on Landsat-8 and 11 classes on Sentinel-2A imagery. The resulted classified maps are presented in Figs. 3 and 4 respectively.

E. Evaluation

RF was tested on the entire study area. We evaluated classification performance using the Overall Accuracy (OA), Producers' Accuracy (PA), Users' Accuracy (UA) and Kappa Coefficient (KC). In order to provide an accuracy assessment of RF classification, we selected a total of 729 validation points for Landsat-8 and 812 points for Sentinel-2A. The accuracy metrics are presented in Tables IV and V.

RF produced slightly higher overall accuracy using Landsat-8 (82,99%) than Sentinel-2A (80,30%). In case of Landsat-8 classification, analyzing the map (Fig. 3) and its accuracy metrics (Table IV), the best results were achieved at water bodies (512), non-irrigated arable land (211) and needle-leaved forest (312). Issues were noticed in two classes: permanent crops (fruit trees and olive trees) and emergent

vegetation. Both of them are confused with shrubs. These classes cover small in size areas and probably the relevant training and validation data are not enough. In reference to Sentinel-2A classification, the main issue is the class of shrubs. It is confused partially with non-irrigated lands where these small in size land parcels are surrounded by shrubs. In addition, low accuracy is recorded in small area classes of emergent vegetation, mineral extraction, and artificial surfaces as well.

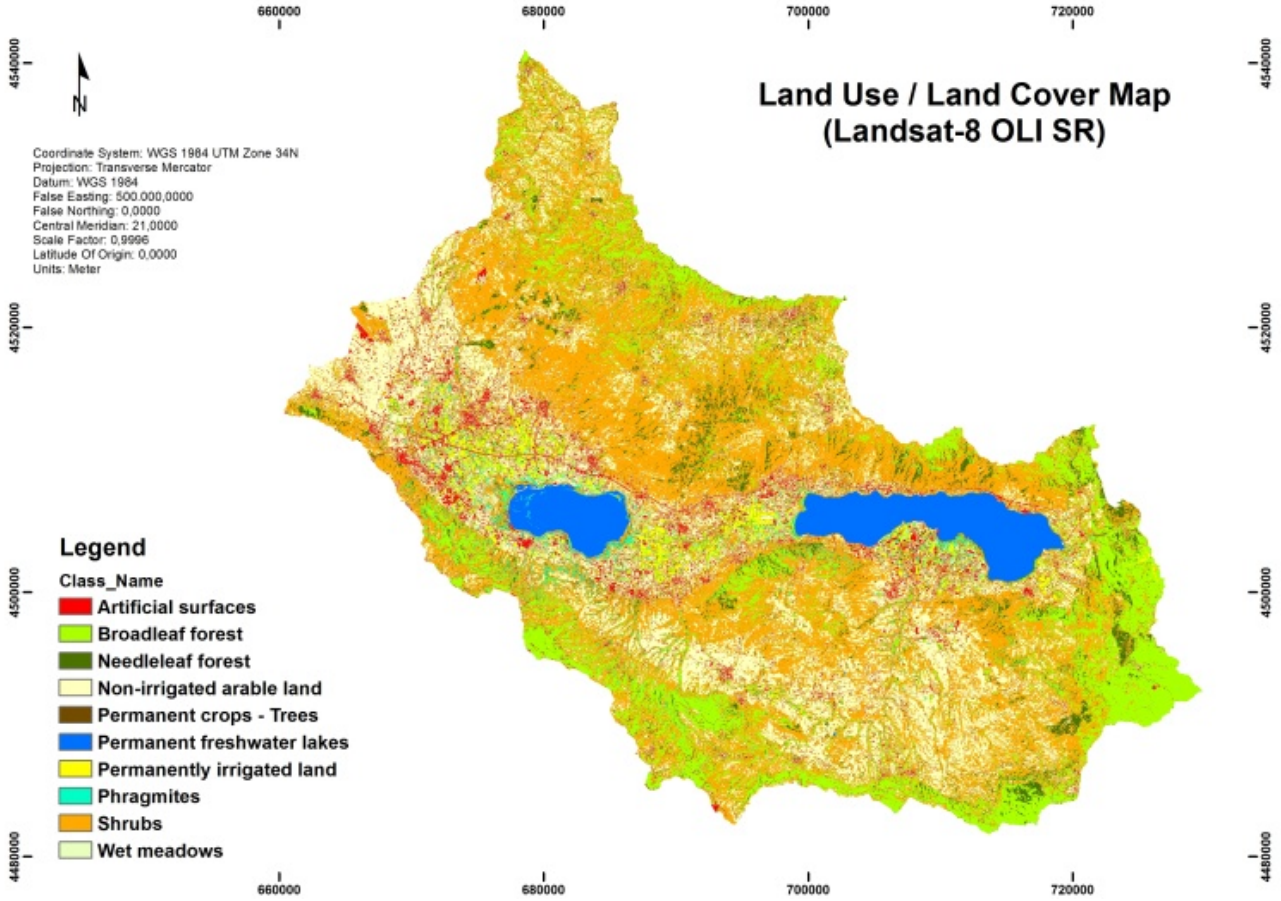

Fig. 3 Land use/land cover map, Landsat-8 OLI SR

TABLE IV
LANDSAT-8 CLASSIFICATION ACCURACY METRICS

Class	PA	UA	KC
Artificial surfaces	85.96%	90.74%	0.8996
Broadleaf forest	78.49%	80.22%	0.7733
Needleleaf forest	91.30%	72.41%	0.7152
Non-irrigated arable land	95.09%	82.01%	0.7683
Permanent crops	22.50%	52.94%	0.5021
Water bodies	100.00%	98.18%	0.9804
Permanently irrigated arable land	83.72%	92.31%	0.9183
Emergent vegetation	66.67%	71.43%	0.7083
Shrubs	82.25%	82.25%	0.7402
Wet meadows	80.00%	80.00%	0.7972

IV. CONCLUSION

Our approach was to integrate a variety of information from higher-accuracy ancillary data with single-date spectral data, and implement land cover classification. Our goal was to evaluate Landsat-8 and Sentinel-2A imagery RF classification in the identification and mapping of land use/land cover types under CLC2018 nomenclature.

TABLE V
SENTINEL-2A CLASSIFICATION ACCURACY METRICS

Class	PA	UA	KC
Artificial surfaces	55.17%	59.26%	0.5775
Broadleaf forest	96.46%	72.19%	0.6769
Mineral extraction	56.25%	69.23%	0.6861
Needleleaf forest	92.68%	97.44%	0.9730
Non-irrigated arable land	83.91%	76.84%	0.6587
Water bodies	100.00%	100.00%	1
Permanently irrigated arable land	91.11%	89.13%	0.8849
Emergent vegetation	64.71%	64.71%	0.6395
Roads	69.57%	76.19%	0.7550
Seasonal streams	62.50%	86.96%	0.8642
Shrubs	65.75%	87.50%	0.8391

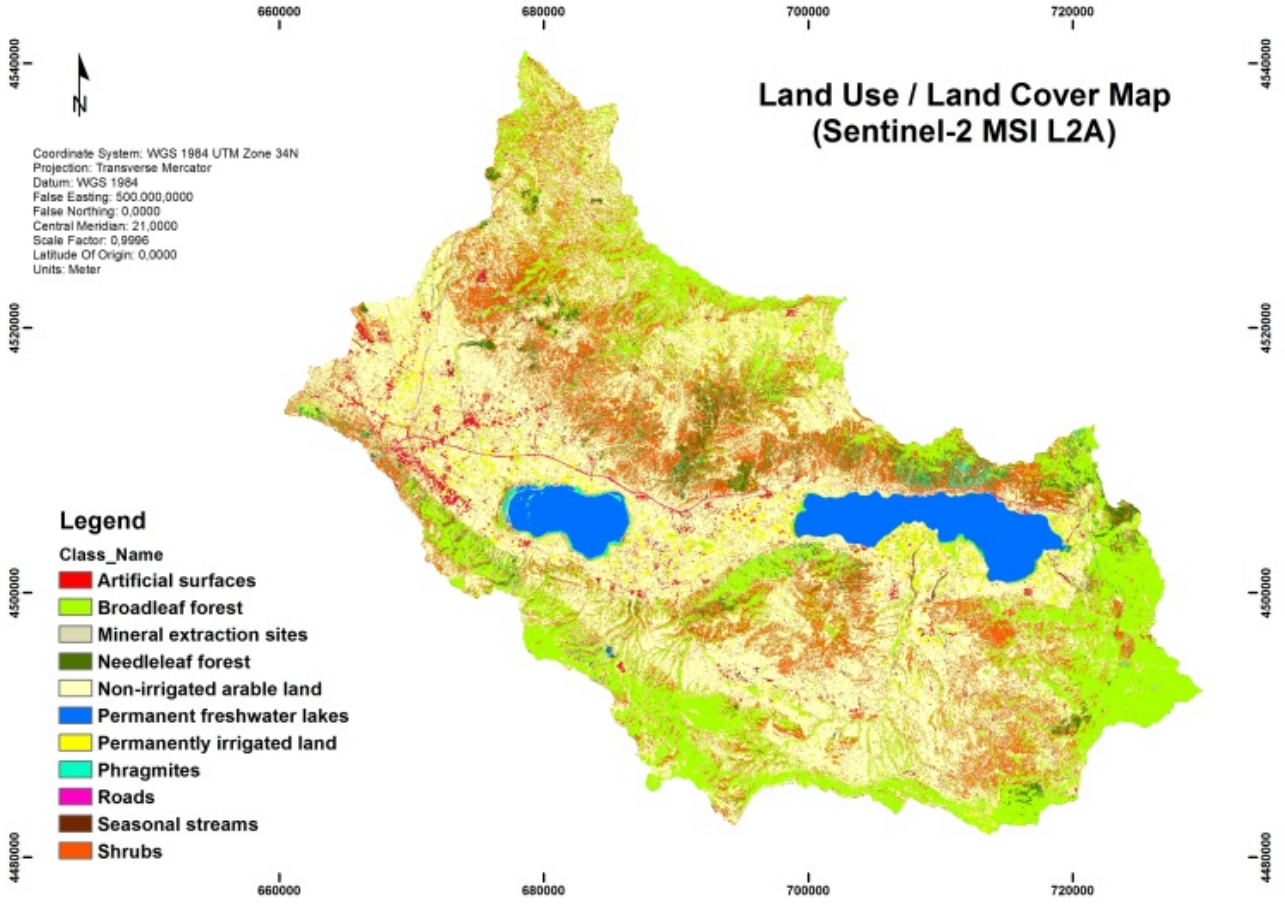

Fig. 4 Land use/land cover map, Sentinel-2A

Based on the results, the achieved overall accuracies are acceptable (> 80%), given the study area is highly heterogeneous. It comprised of various land use/land cover types, which distributed unevenly across the study area. Different patterns of agricultural lands (fallow lands, wet fields around wetlands and small parcels surrounded by shrubs), wetlands (mixed shrubs, mixed high reeds formations and shrubs, wet meadows and marshes), and forest types (mixed broadleaf/shrubs, degraded broadleaf forests, mixed shrub/natural grasslands, and riparian forests) span the entire study area.

The observed confusion was caused by factors, such as: a) difficulties to identify the dominant land use/land cover type, b) difficulties in determining the exact land use/land cover type, and c) lack of VHR reference orthoimagery at the date of satellite image acquisition. We point out that available land use/land cover reference data cover just a portion of the study area. Analyzing the sensor's effect on classification accuracy, better OA results (3%) were obtained for the OLI sensor than MSI, despite its lower spatial resolution. Additional information is needed to increase the accuracy and consistency of land cover mapping.

We believe that seasonal time-series spectral information may improve land use/land cover classification. Our research contributes to the efforts of automated CLC evolution in the near future.

References

[1] Büttner, G., 2014. Corine Land Cover and Land Change Products, In Proc. Land Use and Land Cover Mapping in Europe: Practices and Trends, I. Manakos and M. Braun, (eds.), p. 3, London.

[2] Kuntz, S., E. Schmeer, M. Jochum, and G. Smith, 2014. Towards an European land cover monitoring service and high-resolution layers. In Remote Sensing and Digital Image Processing, vol. 18, pp. 43–52, Springer International Publishing, https://doi.org/10.1007/978-94-007-7969-3_4.

[3] Pflugmacher, D., A. Rabe, M. Peters, and P. Hostert, 2019. Mapping pan-European land cover using Landsat spectral-temporal metrics and the European LUCAS survey, Remote Sens. Environ., https://doi.org/10.1016/j.rse.2018.12.00.

[4] Maxwell, A.E., A.T. Warner, and F. Fang, 2018. Implementation of machine-learning classification in remote sensing: An applied review. In Int. J. Remote Sens., https://doi.org/10.1080/01431161.2018.1433343.

[5] Breiman, L., 2001. Random Forests, Kluwer Academic Publishers, 45, 5–32.

[6] Rodriguez-Galiano, F.V., B. Ghimire, J. Rogan, M. Chica-Olmo, and J.P. Rigol-Sanchez, 2012. An assessment of the effectiveness of a random forest classifier for land-cover classification, ISPRS J. Photogram. Remote Sens. 67:93–104, https://doi:10.1016/j.isprsjprs.2011.11.002.

[7] Zeferino, B.L., de Souza, T.F.L., do Amaral, H.C., Filho, F.I.E., de Oliveira, S. T., 2020. Does environmental data increase the accuracy of land use and land cover classification? Int. J. Appl. Earth Obs. Geoinf. 91, 102128. https://doi.org/10.1016/j.jag.2020.102128.

[8] Abdulhakim, M. A., 2020. Land cover and land use classification performance of machine learning algorithms in a boreal landscape using Sentinel-2 data, GIScience Remote Sens., 57:1, 1-20, https://doi.org/10.1080/15481603.2019.1650447.

[9] Brown, J. F., J. H. Tollerud, P. C. Barber, Q. Zhou, L. J. Dwyer, E. J. Vogelmann, R. T. Loveland, E. C. Woodcock, V. S. Stehman, Z. Zhu,

W. B. Pengra, K. Smith, A. J. Horton, G. Xian, F. R. Auch, L.T. Sohl, L. K. Sayler, L. A. Gallant, D. Zelenak, and J. Rover, 2020. Lessons learned implementing an operational continuous United States national land change monitoring capability: The Land Change Monitoring, Assessment, and Projection (LCMAP) approach, Remote Sens. Environ., 238, https://doi.org/10.1016/j.rse.2019.111356.

[10] Vogelmann, J. E., M.S. Howard, L. Yang, R. C. Larson, K. B. Wylie, and N. Van Driel, 2001. Completion of the 1990s national land cover data set for the conterminous United States from Landsat Thmatic Mapper data and ancillary data sources, ASPRS, vol. 67 (6), 11p.

[11] Stehman, S. V., and G. M. Foody, 2019. Key issues in rigorous accuracy assessment of land cover products, Rem. Sens. Environ. 231, 111199, https://doi.org/10.1016/j.rse.2019.05.018.

[12] Foody, G. M., P. Mahesh, D. Rocchini, X. C. Garzon-Lopez, and L. Bastin, 2016. The Sensitivity of Mapping Methods to Reference Data Quality: Training Supervised Image Classifications with Imperfect Reference Data, ISPRS Intern. J. Geo-Inf., 5, 11, 199, https://doi.org/10.3390/ijgi5110199.

[13] Landsat-8 C2L2 images courtesy of the U.S. Geological Survey, http://earthexplorer.usgs.gov.

[14] Copernicus Sentinel data 2018 for Sentinel data, European Space Agency–ESA, produced from ESA remote sensing data, https://scihub.copernicus.eu/dhus/#/home.

[15] Drusch, M., U. Del Bello, S. Carlier, O. Colin, V. Fernandez, F. Gascon, B. Hoersch, C. Isola, P. Laberinti, P. Martimort, A. Meygret, F. Spoto, O. Sy, F. Marchese, and P. Bargellini, 2012. Sentinel-2: ESA's Optical High-Resolution Mission for GMES Operational Services, J. Remote. Sens. Environ., 120, 25–36, https://doi.org/10.1016/j.rse.2011.11.026.

[16] Zheng, H., P. Du, J. Chen, J. Xia, E. Li, Z. Xu, X. Li, and N. Yokoya, 2017. Performance evaluation of downscaling sentinel-2 imagery for land use and land cover classification by spectral-spatial features. Rem. Sens, 9(12), 1274, https://doi.org/10.3390/rs9121274.

[17] Tóth, K. and A. Kucas, 2016. Spatial information in European agricultural data management. Requirements and interoperability supported by a domain model, Land Use Policy, 57, 64–79, http://dx.doi.org/10.1016/j.landusepol.2016.05.023.

[18] Vogiatzis, M., 2008. Cadastral Mapping of Forestlands in Greece, Photogramm. Eng. Remote Sens., 74:39-46, https://doi.org/10.14358/PERS.74.1.39.

[19] Dabija, A., M. Kluczek, B. Zagajewski, E. Raczko, M. Kycko, Al-Sulttani, A.H. A. Tardà, L. Pineda and J. Corbera, 2021. Comparison of support vector machines and random forests for corine land cover mapping, Remote Sens., 13, 1–35, https://doi.org/10.3390/rs13040777.

[20] Thinh, T.V., P.C. Duong, K.N. Nasahara, and T. Tadono, 2019. How does land use/land cover map's accuracy depend on number of classification classes? SOLA, 15:28-31, https://doi.org/10.2151/sola.2019-006.

[21] UN, 2015. Transforming our world: the 2030 Agenda for Sustainable Development, https://www.un.org/sustainabledevelopment/development-agenda/.

[22] Ramsar Sites Information Service, https://rsis.ramsar.org/ris/57.

[23] Government Gazette No. B-4432, 2017. Revision of National Catalogue of Sites of European Ecological Network Natura2000, Ministry of Environment and Energy, Athens, Greece.